Physical interpretation and evaluation of the Kohn-Sham and Dyson components of the epsilon-I relations between the Kohn-Sham orbital energies and the ionization potentials

Gritsenko, O.V.; Braida, B.; Baerends, E.J.

published in
Journal of Chemical Physics
2003

DOI (link to publisher)
10.1063/1.1582839

document version
Publisher's PDF, also known as Version of record

Physical interpretation and evaluation of the Kohn–Sham and Dyson components of the $\epsilon - I$ relations between the Kohn–Sham orbital energies and the ionization potentials

O. V. Gritsenko, B. Braïda,[a] and E. J. Baerends
Section Theoretical Chemistry, Vrije Universiteit, De Boelelaan 1083, 1081 HV Amsterdam, The Netherlands

(Received 29 January 2003; accepted 24 April 2003)

Theoretical and numerical insight is gained into the $\epsilon - I$ relations between the Kohn–Sham orbital energies ϵ_i and relaxed vertical ionization potentials (VIPs) I_j, which provide an analog of Koopmans' theorem for density functional theory. The Kohn–Sham orbital energy ϵ_i has as leading term $-n_i I_i - \Sigma_{j\in\Omega_s(i)} n_j I_j$, where I_i is the primary VIP for ionization $(\phi_i)^{-1}$ with spectroscopic factor (proportional to the intensity in the photoelectron spectrum) n_i close to 1, and the set $\Omega_s(i)$ contains the VIPs I_j that are satellites to the $(\phi_i)^{-1}$ ionization, with small but non-negligible n_j. In addition to this "average spectroscopic structure" of the ϵ_i there is an electron-shell step structure in ϵ_i from the contribution of the response potential v_{resp}. Accurate KS calculations for prototype second- and third-row closed-shell molecules yield valence orbital energies $-\epsilon_i$, which correspond closely to the experimental VIPs, with an average deviation of 0.08 eV. The theoretical relations are numerically investigated in calculations of the components of the $\epsilon - I$ relations for the H_2 molecule, and for the molecules CO, HF, H_2O, HCN. The derivation of the $\epsilon - I$ relations employs the Dyson orbitals (the n_i are their norms). A connection is made between the KS and Dyson orbital theories, allowing the spin-unrestricted KS xc potential to be expressed with a statistical average of individual xc potentials for the Dyson spin–orbitals as leading term. Additional terms are the correction $v_{c,\mathrm{kin},\sigma}$ due to the correlation kinetic effect, and the "response" $v_{\mathrm{resp},\sigma}$, related to the correction to the energy of $(N-1)$ electrons due to the correlation with the reference electron. © *2003 American Institute of Physics.* [DOI: 10.1063/1.1582839]

I. INTRODUCTION

The fundamental importance of the Kohn–Sham density functional theory (KS-DFT) (Refs. 1–3) is based on the fact, that it offers an exact independent-particle approach in many-electron theory. It is exact in the sense, that the exact density of the interacting system is delivered with the KS noninteracting system. In the spin-density version of DFT (SDFT) (Refs. 4–6) the exact spin-density ρ_σ of the highest state $(M=S)$ of a multiplet $\{\Psi^{NSM}\}$ is produced with the N_σ lowest KS spin–orbitals $\phi_{i\sigma}$,

$$\rho_\sigma(\mathbf{r}_1) = \sum_i^{N_\sigma} |\phi_{i\sigma}(\mathbf{r}_1)|^2. \tag{1.1}$$

From a general point of view, the orbitals $\phi_{i\sigma}$ can be defined meaningfully as the Dyson orbitals of the KS noninteracting system. Indeed, for the interacting system the Dyson spin–orbitals $d_{i\sigma}$ are defined conventionally[7] with the overlap of a pure N electron ground state Ψ_0^{NSS} (we consider the "top" component of the multiplet $\{\Psi^{NSM}\}$ of degenerate states with the spin S) with pure $(N-1)$ electron states $\Psi_i^{(N-1)S'M'}$,

$$d_{i\sigma}(\mathbf{r}_1)\sigma(s_1) = \sqrt{N}\int \Psi_i^{(N-1)S'M'*}(\mathbf{x}_2,\ldots,\mathbf{x}_N) \times \Psi_0^{NSS}(\mathbf{x}_1,\ldots,\mathbf{x}_N)\,d\mathbf{x}_2\cdots d\mathbf{x}_N \quad (M'=S-m_\sigma). \tag{1.2}$$

Note, that in the literature the Dyson orbitals are also called "generalized overlap amplitudes." Throughout the paper for any wave function Ψ^{NSM} the first superscript index N is the number of electrons, the second one S is its spin, and the third one M is its eigenvalue for the operator $\hat{S}_z$. The index i runs over all the ion states, each ion state is characterized by a specific total spin S' and z-component M'. In Eq. (1.2) m_σ is the eigenvalue of $\hat{S}_z$ for the functions $\sigma(s_1)$, $\hat{S}_z\sigma(s_1) = m_\sigma\sigma(s_1)$, $m_\alpha = +1/2$, $m_\beta = -1/2$. Note that only ion states $\Psi_i^{(N-1)S'M'}$ for which $M' = S \pm 1/2$ and $S - 1/2 \leqslant S' \leqslant S + 1/2$ correspond to nonzero Dyson orbitals.

In turn, the KS spin–orbitals $\phi_{i\sigma}$ can be defined with the overlap of the corresponding noninteracting states,

$$\phi_{i\sigma}(\mathbf{r}_1)\sigma(s_1) = \sqrt{N}\int \Psi_{s,(S-m_\sigma),i}^{(N-1)*}(\mathbf{x}_2,\ldots,\mathbf{x}_N) \times \Psi_{s,(M=S)}^{N}(\mathbf{x}_1,\ldots,\mathbf{x}_N)\,d\mathbf{x}_2\cdots d\mathbf{x}_N. \tag{1.3}$$

In Eq. (1.3) $\Psi_{s,(M=S)}^{N}$ is the KS determinant with N_α α-electrons and N_β β-electrons, corresponding to the interacting state Ψ^{NSS}, and the $(N-1)$ electron states $\Psi_{s,(M=S-m_\sigma),i}^{(N-1)}$ result from removal of the orbital $\phi_{i\sigma}$ from

[a]Also at Laboratoire de Chimie Physique, Groupe de Chimie Théorique, Université Paris-Sud, 91405 Orsay, France. Present address: ICMAB-CSIC, Campus de la UAB, 08193 Bellaterra, Barcelona, Spain.

$\Psi^N_{s,(M=S)}$. These states are not necessarily eigenstates of $\hat{S}^2$, therefore we only specify the eigenvalue of $\hat{S}_z$ in the subscript. We note that in the noninteracting system only ''primary'' ionizations (out of occupied orbitals without any other orbital excitation to virtual orbitals) have nonzero Dyson orbitals, which are identical to the Kohn–Sham orbitals.

Furthermore, the orbitals $d_{i\sigma}$ have minus the ionization energies [or vertical ionization potentials (VIPs)] of the interacting system $-I_i^{S'}=E_0^{NS}-E_i^{(N-1)S'}$ as their eigenvalues in the one-electron Dyson equations,

$$\{-\tfrac{1}{2}\nabla^2+v_{\rm ext}(\mathbf{r}_1)+v_{\rm Coul}(\mathbf{r}_1)+\hat{\Sigma}_{{\rm xc},\sigma}(I_i^{S'})\}d_{i\sigma}(\mathbf{r}_1) = -I_i^{S'}d_{i\sigma}(\mathbf{r}_1), \tag{1.4}$$

where $v_{\rm ext}$ is the external potential, $v_{\rm Coul}$ is the Hartree potential of the electrostatic electron repulsion of the ground state electron density, and $\hat{\Sigma}_{{\rm xc},\sigma}$ is the nonlocal xc self-energy operator. In their turn, the KS orbitals $\phi_{i\sigma}$ have ionization energies of the noninteracting system $\epsilon_{i\sigma}=E^N_{s,(M=S)}-E^{(N-1)}_{s,(S-m_\sigma),i}$ as their eigenvalues in the KS one-electron equations,

$$\{-\tfrac{1}{2}\nabla^2+v_{\rm ext}(\mathbf{r}_1)+v_{\rm Coul}(\mathbf{r}_1)+v_{{\rm xc},\sigma}(\mathbf{r}_1)\}\phi_{i\sigma}(\mathbf{r}_1) = \epsilon_{i\sigma}\phi_{i\sigma}(\mathbf{r}_1), \tag{1.5}$$

where $v_{{\rm xc},\sigma}$ is the local, state-independent xc potential. Note that, unlike in the finite, independent-particle representation (1.1), the same spin-density ρ_σ is expressed with all ''interacting'' Dyson orbitals $d_{i\sigma}$,

$$\rho_\sigma(\mathbf{r}_1)=\sum_i^\infty |d_{i\sigma}(\mathbf{r}_1)|^2. \tag{1.6}$$

The physical meaning of the KS orbital energies $\epsilon_{i\sigma}$ is provided by an analog of Koopmans theorem established recently in Refs. 8 and 9. It is based on the exact relations between the energies ϵ_i of $H=N/2$ occupied orbitals ϕ_i and VIPs I_j,

$$\boldsymbol{\epsilon}=-\mathbf{M}^{-1}\mathbf{P}\mathbf{I}+\mathbf{M}^{-1}\boldsymbol{\epsilon}^{\rm resp},$$

$$M_{ij}=2\int\frac{|\phi_i(\mathbf{r})|^2|\phi_j(\mathbf{r})|^2}{\rho(\mathbf{r})}d\mathbf{r}\quad (H\times H\ \text{matrix}), \tag{1.7}$$

$$P_{ij}=2\int\frac{|\phi_i(\mathbf{r})|^2|d_j(\mathbf{r})|^2}{\rho(\mathbf{r})}d\mathbf{r}\quad (H\times\infty\ \text{matrix}).$$

These equations were derived for closed-shell systems. The infinite-dimensional column vector $\mathbf{I}$ contains all ionization energies, which are ordered in the same way as the set of Dyson orbitals (i.e., the columns of $\mathbf{P}$), namely the primary ionizations come first. The primary ionizations are those that can be described in good approximation by a Koopmans' configuration, i.e., a single orbital ionization. When there is strong correlation in the ground state or in the ionized state, it may not be possible to identify H ionizations unambiguously as primary ones. Such molecules are not included in this study. The H-dimensional column vector $\boldsymbol{\epsilon}^{\rm resp}$ contains the matrix elements $\epsilon_j^{\rm resp}=\int|\phi_j(\mathbf{r}_1)|^2v_{\rm resp}(\mathbf{r}_1)d\mathbf{r}_1$ of the ''response'' potential for the occupied KS orbitals.[3,10,11] A qualitative interpretation of Eq. (1.7) made in Ref. 8 allows us to identify the KS orbital energies ϵ_i as approximate but rather accurate *relaxed* VIPs I_i,

$$\epsilon_i\approx -I_i. \tag{1.8}$$

The quality of this approximation appears to be high for outer valence orbitals and it becomes an exact identity for the highest occupied molecular orbital (HOMO).

In this paper a comparative theoretical and numerical study of the Kohn–Sham and Dyson orbitals is carried out and calculation of various components of the relations (1.7) are performed for prototype molecules. In Sec. II a connection is established between the one-electron equations for the Dyson spin–orbitals $d_{i\sigma}$ and for the Kohn–Sham orbitals. The equations for the Dyson spin–orbitals $d_{i\sigma}$ and the Schrödinger equation for the square root of the spin-density ρ_σ are derived as limiting cases of universal equations for partial spin-densities of an arbitrary subset of the Dyson spin–orbitals.

Comparison of these equations with the spin-unrestricted KS one-electron equations allows to establish a relation between the xc potentials (operators) for Dyson and KS orbitals. In Sec. III the orbital energies ϵ_i are obtained with accurate KS potentials constructed from *ab initio* densities for some prototype closed-shell molecules of elements of the first three periods and they are compared with the experimental VIPs I_i. The accurate $-\epsilon_i$ of the valence orbitals provide a very good estimate of the corresponding I_i, with average deviation of only 0.08 eV. Section IV presents a benchmark calculation for H_2 of the KS and Dyson components of the relations (1.7), which provides a numerical confirmation of these relations. In Sec. V the ingredients of Eq. (1.7), the Dyson orbitals d_i, the matrices $\mathbf{M}$ and $\mathbf{P}$, and the components $\mathbf{M}^{-1}\mathbf{P}\mathbf{I}$ and $\mathbf{M}^{-1}\boldsymbol{\epsilon}^{\rm resp}$ are obtained with *ab initio* and accurate KS calculations for the molecules CO, HF, H_2O, HCN. In Sec. VI the implications of the present results for DFT are discussed and the conclusions are drawn.

II. UNIVERSAL EQUATION FOR PARTIAL SPIN-DENSITIES

The road to a meaningful comparison of the one-electron equations for the KS and Dyson orbitals passes through the Schrödinger-type equation for the square root of the spin-density,

$$\{-\tfrac{1}{2}\nabla^2+v_{{\rm eff},\sigma}(\mathbf{r}_1)\}\sqrt{\rho_\sigma(\mathbf{r}_1)}=\mu_\sigma\sqrt{\rho_\sigma(\mathbf{r}_1)}. \tag{2.1}$$

In this section we shall show that both Eq. (1.4) for $d_{i\sigma}$ and Eq. (2.1) for $\sqrt{\rho_\sigma}$ are just the limiting cases of an universal equation for the square root of the partial spin-density ρ^p_σ,

$$\rho^p_\sigma(\mathbf{r}_1)=\sum_{j\in\Omega_p}|d_{j\sigma}(\mathbf{r}_1)|^2 \tag{2.2}$$

of any arbitrary subset $\{d_{j\sigma}, j\in\Omega_p\}$ of Dyson spin–orbitals. In order to derive this equation, we expand the N electron ground state Ψ_0^{NSS} in terms of $(N-1)$ electron states $\Psi_i^{(N-1)S'M'}$ and the corresponding Dyson orbitals $d_{i\sigma}(\mathbf{r}_1)\sigma(s_1)$,

$$\Psi_0^{NSS}(\mathbf{x}_1,\ldots,\mathbf{x}_N)=\frac{1}{\sqrt{N}}\sum_{\sigma=\alpha,\beta}\sum_{S'=(S-m_\sigma)}^{S+1/2}\sum_{i[S'(S-m_\sigma)]}d_{i\sigma}(\mathbf{r}_1)\times\sigma(s_1)\Psi_i^{(N-1)S'(S-m_\sigma)}(\mathbf{x}_2,\ldots,\mathbf{x}_N), \tag{2.3}$$

where $i[S'(S-m_\sigma)]$ means that the index i only runs over those ion states $\Psi_i^{(N-1)S(i)M(i)}$ for which the total spin $S(i)=S'$ and the $\hat{S}_z$-eigenvalue $M(i)=S-m_\sigma$. It is also possible to expand the wave function using the spin-resolved conditional probability amplitudes

$$\Phi_\sigma(\mathbf{x}_2\cdots\mathbf{x}_N|\mathbf{r}_1)=\Psi(\mathbf{r}_1\sigma,\mathbf{x}_2\cdots\mathbf{x}_N)/\sqrt{\rho_\sigma(\mathbf{r}_1)/N},$$
$$\Psi_0^{NSS}(\mathbf{x}_1,\ldots,\mathbf{x}_N)=\sum_{\sigma=\alpha,\beta}\sqrt{\frac{\rho_\sigma(\mathbf{r}_1)}{N}}\Phi_\sigma(\mathbf{x}_2\cdots\mathbf{x}_N|\mathbf{r}_1)\sigma(s_1), \tag{2.4}$$

Φ_σ is an $(N-1)$-electron wave function, the square of which is the probability to find electrons 2,...,N with spatial and spin coordinates $\mathbf{x}_2=\mathbf{r}_2,s_2,\ldots,\mathbf{x}_N=\mathbf{r}_N,s_N$, if electron 1 is at the position $\mathbf{r}_1$ with spin σ. It follows from Eqs. (2.3) and (2.4), that for the minor spin (β) only the states $\Psi_i^{(N-1)(S+1/2)(S+1/2)}$ with $S'=(S+1/2)$, $M'=(S+1/2)$ contribute to Φ_β, while for the major spin (α) the states $\Psi_i^{(N-1)(S\pm1/2)(S-1/2)}$ with $M'=S-1/2$ and both $S'=S+1/2$ and $S'=S-1/2$ contribute to Φ_α. Then, by analogy with Φ_σ, we introduce the partial spin-amplitude Φ_σ^p,

$$\Phi_\sigma^p(\mathbf{x}_2\cdots\mathbf{x}_N|\mathbf{r}_1)=\frac{1}{\sqrt{\rho_\sigma^p(\mathbf{r}_1)}}\sum_{j\in\Omega_p}d_{j\sigma}(\mathbf{r}_1)\Psi_j^{(N-1)S'(j)M'(j)}\times(\mathbf{x}_2\cdots\mathbf{x}_N)(M'(j)=S-m_\sigma), \tag{2.5}$$

which includes the Dyson orbitals $\{d_{j\sigma},j\in\Omega_p\}$ contributing to ρ_σ^p of (2.2) and the parent $(N-1)$ electron states $\Psi_j^{(N-1)S'(j),M'(j)}$,$(M'(j)=S-m_\sigma)$.

With Eqs. (2.3)–(2.5), one can derive an effective one-electron equation for $\sqrt{\rho_\sigma^p}$ from the Schrödinger equation $\hat{H}^N\Psi_0^{NSS}=E_0^{NS}\Psi_0^{NSS}$ by partitioning of its (spin-free) Hamiltonian $\hat{H}^N$ into the $(N-1)$ electron Hamiltonian $\hat{H}^{N-1}$ and the remainder,

$$\hat{H}^N=-\frac{1}{2}\nabla_1^2+v_{\text{ext}}(\mathbf{r}_1)+\sum_{j=2}^N\frac{1}{|\mathbf{r}_1-\mathbf{r}_j|}+\hat{H}^{N-1}.$$

For each spin σ we also subtract from both sides of the Schrödinger equation the term $E_{p0}^{(N-1)(\sigma)}\Psi_0^{NSS}$, where $E_{p0}^{(N-1)(\sigma)}$ is the lowest energy for the states $\Psi_j^{(N-1)S'(j),M'(j)}$ which contribute to Φ_σ^p. Inserting expansion (2.3) and the partitioning of the Hamiltonian in the Schrödinger equation with $E_{p0}^{(N-1)(\sigma)}\Psi_0^{NSS}$ subtracted, and then multiplying by the partial spin-amplitude $\Phi_\sigma^p(\mathbf{x}_2,\ldots,\mathbf{x}_N|\mathbf{r}_1)\sigma(s_1)$ and integrating over $s_1,\mathbf{x}_2,\ldots,\mathbf{x}_N$, we obtain an exact equation for the square root of the partial spin-density ρ_σ^p,

$$\{-\tfrac{1}{2}\nabla^2+v_{\text{ext}}(\mathbf{r}_1)+v_{\text{kin},\sigma}^p(\mathbf{r}_1)+v_\sigma^{N-1(p)}(\mathbf{r}_1)+\hat{W}_{\text{cond},\sigma}^{(p)}\}\times\sqrt{\rho_\sigma^p(\mathbf{r}_1)}=\mu_\sigma^p\sqrt{\rho_\sigma^p(\mathbf{r}_1)}, \tag{2.6}$$

where $\mu_\sigma^p=E_0^{NS}-E_{p0}^{(N-1)(\sigma)}$. In Eq. (2.6), $v_{\text{kin},\sigma}^p$ and $v_\sigma^{N-1(p)}$ are local potentials defined in terms of the partial amplitude Φ_σ^p. In particular, $v_{\text{kin},\sigma}^p$ is the kinetic contribution,

$$v_{\text{kin},\sigma}^p(\mathbf{r}_1)=\langle\Phi_\sigma^p|-\tfrac{1}{2}\nabla_1^2|\Phi_\sigma^p\rangle \tag{2.7}$$

(the brackets $\langle\ \rangle$ denote integration over $s_1,\mathbf{x}_2,\ldots,\mathbf{x}_N$, *not* over $\mathbf{r}_1$) and the potential $v_\sigma^{N-1(p)}$ is determined with the expectation value of the $(N-1)$ electron Hamiltonian $\hat{H}^{N-1}$,

$$v_\sigma^{N-1(p)}(\mathbf{r}_1)=\langle\Phi_\sigma^p|\hat{H}^{N-1}|\Phi_\sigma^p\rangle-E_{p0}^{(N-1)(\sigma)}=\sum_{j\in\Omega_p}\frac{|d_{j\sigma}(\mathbf{r}_1)|^2}{\rho_\sigma^p(\mathbf{r}_1)}(E_j^{(N-1)S'(j)}-E_{p0}^{(N-1)(\sigma)}). \tag{2.8}$$

The nonlocal operator $\hat{W}_{\text{cond},\sigma}^{(p)}$ represents in Eq. (2.6) the potential effect of the electron–electron interaction, it is defined in terms of both partial Φ_σ^p and total Φ_σ conditional probability spin-amplitudes and its action on $\sqrt{\rho_\sigma^p}$ is defined as follows:

$$\hat{W}_{\text{cond},\sigma}^{(p)}\sqrt{\rho_\sigma^p(\mathbf{r}_1)}=\langle\Phi_\sigma^p|\sum_{j=2}^N\frac{1}{|\mathbf{r}_1-\mathbf{r}_j|}|\Phi_\sigma\rangle\sqrt{\rho_\sigma(\mathbf{r}_1)}. \tag{2.9}$$

Thus, $\hat{W}_{\text{cond},\sigma}^{(p)}$ can be considered as a "superexchange" operator acting on the "superorbital" $\sqrt{\rho_\sigma^p}$, it takes this "superorbital" and replaces it with the square root of the total spin-density $\sqrt{\rho_\sigma}$. Subtracting from $\hat{W}_{\text{cond},\sigma}^{(p)}$ the Hartree potential of the electrostatic electron repulsion v_{Coul}, we define the partial xc-hole operator $\hat{W}_{\text{xc},\sigma}^{\text{hole}(p)}=\hat{W}_{\text{cond},\sigma}^{(p)}-v_{\text{coul}}(\mathbf{r}_1)$, so that the universal equation (2.6) for partial spin-densities assumes the final form,

$$\{-\tfrac{1}{2}\nabla^2+v_{\text{ext}}(\mathbf{r}_1)+v_{\text{kin},\sigma}^p(\mathbf{r}_1)+v_\sigma^{N-1(p)}(\mathbf{r}_1)+v_{\text{Coul}}(\mathbf{r}_1)+\hat{W}_{\text{xc},\sigma}^{\text{hole}(p)}\}\sqrt{\rho_\sigma^p(\mathbf{r}_1)}=\mu_\sigma^p\sqrt{\rho_\sigma^p(\mathbf{r}_1)}. \tag{2.10}$$

If only a single Dyson spin–orbital $d_{j\sigma}$ is taken in Eq. (2.2), the potentials $v_\sigma^{N-1(p)}$ and $v_{\text{kin},\sigma}^p$ vanish in the corresponding Eq. (2.10) and it turns into the Dyson equation represented as follows:

$$\{-\tfrac{1}{2}\nabla^2+v_{\text{ext}}(\mathbf{r}_1)+v_{\text{Coul}}(\mathbf{r}_1)+\hat{W}_{\text{xc},\sigma}^{\text{hole},j}\}d_{j\sigma}(\mathbf{r}_1)=-I_jd_{j\sigma}(\mathbf{r}_1). \tag{2.11}$$

In Eq. (2.11) the action of the operator $\hat{W}_{\text{xc},\sigma}^{\text{hole},j}$ on $d_{j\sigma}$ is defined as

$$\hat{W}_{\text{xc},\sigma}^{\text{hole},j}d_{j\sigma}(\mathbf{r}_1)=\langle\Psi_j^{(N-1)}|\sum_{k=2}^N\frac{1}{|\mathbf{r}_1-\mathbf{r}_k|}|\Phi_\sigma\rangle\sqrt{\rho_\sigma(\mathbf{r}_1)}-v_{\text{Coul}}(\mathbf{r}_1)d_{j\sigma}(\mathbf{r}_1). \tag{2.12}$$

Comparison of Eq. (2.11) with the standard form (1.4) of the Dyson equation allows to identify the action of the operator $\hat{W}_{\text{xc},\sigma}^{\text{hole},j}$ with that of the xc self-energy operator $\hat{\Sigma}_{\text{xc}}$,

$$\hat{W}_{\text{xc},\sigma}^{\text{hole},j}d_{j,\sigma}=\hat{\Sigma}_{\text{xc}}(I_j)d_{j,\sigma}. \tag{2.13}$$

For the benefit of further analysis we rewrite Eq. (2.11) with the multiplicative state-dependent potential $v_{\text{xc},\sigma}^{\text{hole},j}(\mathbf{r}_1)$,

$$\{-\tfrac{1}{2}\nabla^2+v_{\rm ext}(\mathbf{r}_1)+v_{\rm Coul}(\mathbf{r}_1)+v_{{\rm xc},\sigma}^{{\rm hole},j}(\mathbf{r}_1)\}d_{j\sigma}(\mathbf{r}_1) = -I_j d_{j\sigma}(\mathbf{r}_1), \tag{2.14}$$

which is defined as

$$v_{{\rm xc},\sigma}^{{\rm hole},j}(\mathbf{r}_1)=\frac{1}{d_{j\sigma}(\mathbf{r}_1)}\hat{W}_{{\rm xc},\sigma}^{{\rm hole},j}d_{j\sigma}(\mathbf{r}_1). \tag{2.15}$$

When all Dyson spin–orbitals $\{d_{j\sigma}\}$ are included in Eq. (2.2), Eq. (2.10) turns to the Schrödinger equation for $\sqrt{\rho_\sigma}$,

$$\{-\tfrac{1}{2}\nabla^2+v_{\rm ext}(\mathbf{r}_1)+v_{{\rm kin},\sigma}(\mathbf{r}_1)+v_\sigma^{N-1}(\mathbf{r}_1)+v_{\rm Coul}(\mathbf{r}_1) +v_{{\rm xc},\sigma}^{\rm hole}(\mathbf{r}_1)\}\sqrt{\rho_\sigma(\mathbf{r}_1)}=\mu_\sigma\sqrt{\rho_\sigma(\mathbf{r}_1)}, \tag{2.16}$$

with $\mu_\sigma=E_0^{NS}-E_0^{(N-1)(\sigma)}$ and the local, state-independent potentials $v_{{\rm kin},\sigma}$, v_σ^{N-1}, $v_{{\rm xc},\sigma}^{\rm hole}$. In particular, the kinetic contribution $v_{{\rm kin},\sigma}$ is[12]

$$v_{{\rm kin},\sigma}(\mathbf{r}_1)=\langle\Phi_\sigma|-\tfrac{1}{2}\nabla_1^2|\Phi_\sigma\rangle, \tag{2.17}$$

and the potential v_σ^{N-1},

$$v_\sigma^{N-1}(\mathbf{r}_1)=\langle\Phi_\sigma|\hat{H}^{N-1}|\Phi_\sigma\rangle-E_0^{(N-1)(\sigma)} =\sum_{S'=(S-m_\sigma)}^{S+1/2}\ \sum_{i[S(i)=S',M(i)=S-m_\sigma]}\frac{|d_{i\sigma}(\mathbf{r}_1)|^2}{\rho_\sigma(\mathbf{r}_1)} \times(E_i^{(N-1)S'}-E_0^{(N-1)(\sigma)}) \tag{2.18}$$

can be expressed as the statistical average over the Dyson spin–orbitals of excitations $(E_i^{(N-1)S'}-E_0^{(N-1)(\sigma)})$ in the $(N-1)$ electron system. The action of the xc-hole operator $\hat{W}_{{\rm xc},\sigma}^{{\rm hole}(p)}$ turns in this case to that of the local potential of the xc-hole $v_{{\rm xc},\sigma}^{\rm hole}$ (Ref. 13) familiar in spin-density functional theory (SDFT),

$$\begin{aligned}&\hat{W}_{{\rm xc},\sigma}^{\rm hole}(\mathbf{r}_1)\sqrt{\rho_\sigma}=v_{{\rm xc},\sigma}^{\rm hole}(\mathbf{r}_1)\sqrt{\rho_\sigma},\\ &v_{{\rm xc},\sigma}^{\rm hole}(\mathbf{r}_1)=\langle\Phi_\sigma|\sum_{j=2}^{N}\frac{1}{|\mathbf{r}_1-\mathbf{r}_j|}|\Phi_\sigma\rangle-v_{\rm Coul}(\mathbf{r}_1)\\ &\qquad=\sum_{\sigma'}\int d\mathbf{r}_2\frac{\rho_{\sigma'}(\mathbf{r}_2)}{|\mathbf{r}_1-\mathbf{r}_2|}[g_{\sigma\sigma'}(\mathbf{r}_1,\mathbf{r}_2)-1],\end{aligned} \tag{2.19}$$

where $g_{\sigma\sigma'}$ is the pair-correlation function. From Eqs. (2.3)–(2.5), (2.12), (2.15), and (2.19) follows, that the xc-hole potential can be expressed as the statistical average of individual xc potentials $v_{{\rm xc},\sigma}^{{\rm hole},j}$ for the Dyson orbitals,

$$v_{{\rm xc},\sigma}^{\rm hole}(\mathbf{r}_1)=\sum_i^\infty\frac{|d_{i\sigma}(\mathbf{r}_1)|^2}{\rho_\sigma(\mathbf{r}_1)}v_{{\rm xc},\sigma}^{{\rm hole},i}(\mathbf{r}_1). \tag{2.20}$$

The xc hole potential is only a part of the total xc potential $v_{{\rm xc},\sigma}$ that features in the KS equations,

$$v_{{\rm xc},\sigma}(\mathbf{r}_1)=v_{{\rm xc},\sigma}^{\rm hole}(\mathbf{r}_1)+v_{c,{\rm kin},\sigma}(\mathbf{r}_1)+v_{{\rm resp},\sigma}(\mathbf{r}_1), \tag{2.21}$$

where $v_{c,{\rm kin},\sigma}$ represents the correlation kinetic effect, and $v_{{\rm resp},\sigma}$ the change of the energy of $(N-1)$ electrons from the ground state energy of the ion to the energy of the conditional amplitude $\Phi_\sigma(\mathbf{x}_2,\ldots,\mathbf{x}_N|\mathbf{r}_1)$ which represents the redistribution of the $(N-1)$-electron system due to the correlation with the reference electron at $\mathbf{r}_1,\sigma$. The potentials $v_{c,{\rm kin},\sigma}$ and $v_{{\rm resp},\sigma}$ have been discussed elsewhere.[3,10,14,15] Then, from Eqs. (2.20) and (2.21) follows the relation between the xc potentials for the KS and Dyson orbitals,

$$v_{{\rm xc},\sigma}(\mathbf{r}_1)=\sum_i^\infty\frac{|d_{i\sigma}(\mathbf{r}_1)|^2}{\rho_\sigma(\mathbf{r}_1)}v_{{\rm xc},\sigma}^{{\rm hole},i}(\mathbf{r}_1)+v_{c,{\rm kin},\sigma}(\mathbf{r}_1) +v_{{\rm resp},\sigma}(\mathbf{r}_1). \tag{2.22}$$

With Eq. (2.22), the xc potential $v_{{\rm xc},\sigma}$ for the KS orbitals $\phi_{i\sigma}$ does not only contain a local hole potential which is a statistical average of individual xc potentials $v_{{\rm xc},\sigma}^{{\rm hole},i}$ for the interacting Dyson orbitals $d_{i\sigma}$ (representing the action of the self-energy operator), but has in addition the terms $v_{c,{\rm kin},\sigma}$ and $v_{{\rm resp},\sigma}$. Equation (2.22) provides an explicit relation between the Kohn–Sham potential and the ''potentials'' (self-energy operator) featuring in the equations for the Dyson orbitals. Neither Eq. (2.22) nor the result of Ref. 16 that the xc Kohn–Sham potential can be considered to be the best local approximation to the exchange-correlation self-energy allow us to make an estimate of how close or remote the correspondence between Kohn–Sham orbitals (only N occupied) and Dyson orbitals (infinite number) actually is, in particular since it is already well known that Hartree–Fock orbitals, Kohn–Sham orbitals, and Dyson orbitals (at least those corresponding to primary ion states) are usually all very similar. We return to this point below.

The response potential plays a crucial role in the $\epsilon-I$ relations [Eq. (1.7)]. This potential has a steplike behavior when going from one shell to another shell in an atom[10] and indeed a rather accurate approximation in the exchange-only case has been provided by Krieger, Li, and Iafrate (KLI),[17] who represented the response part of the exchange potential as the statistical average over the occupied KS orbitals ϕ_i of the orbital ''steps'' w_i,

$$v_{\rm resp}(\mathbf{r}_1)\cong\sum_i^{N/2}\frac{2|\phi_i(\mathbf{r}_1)|^2}{\rho(\mathbf{r}_1)}w_i, \tag{2.23}$$

which exhibits the step structure of $v_{\rm resp}$.[3] Inserting Eq. (2.23) in Eq. (1.7), one obtains

$$\boldsymbol{\epsilon}\cong-\mathbf{M}^{-1}\mathbf{P}\mathbf{I}-\mathbf{w}. \tag{2.24}$$

We will verify in the next section for a series of prototype closed shell molecules that the KS orbital energies indeed approximate quite closely the experimental vertical IPs (for valence levels). Then in the next sections we will further analyze the relations (1.7) and (2.24). In particular the correspondence between occupied Kohn–Sham orbitals and Dyson orbitals belonging to primary ionizations (characterized by a single orbital ionization as leading term in the wave function), and Dyson orbitals of satellites will be discussed in order to provide an understanding of the structure of the matrices $\mathbf{M}$ and $\mathbf{P}$ (hence $\mathbf{M}^{-1}\mathbf{P}$). This is required to arrive at a full explanation of how the relations (1.7) can lead to the ''empirical'' finding that $\epsilon_i\approx I_i$.

TABLE I. Comparison of the KS, HF, and GGA-BP orbital energies $-\epsilon_i$ (eV) with experimental vertical ionization potentials (the corresponding references are indicated in the table). AAD are the average absolute differences between the KS orbital energies and the VIPs for either the upper valence levels, AAD(val) or lower valence and core levels, AAD(inner). For BP in parentheses are the sum $(\epsilon_H + I_H)$ for the HOMO, the orbital energies shifted by this amount for the other orbitals, and AADs for the shifted orbital energies.

	MO	HF	GGA-BP	KS	Expt.
Molecule	MO	$-\epsilon_i$	$-\epsilon_i$	$-\epsilon_i$	I_i
CO[a–e]	5σ	15.12	9.18(4.83)	14.01	14.01
	1π	17.42	11.95(16.78)	16.80	16.91
	4σ	21.94	14.27(19.10)	19.37	19.72
AAD(val)		1.28	5.08(0.25)	0.15	
	3σ	41.47	29.47(34.29)	34.70	38.3
	2σ	309.17	272.50(277.33)	279.27	296.21
	1σ	562.36	513.53(518.37)	519.92	542.55
AAD(inner)		11.98	20.52(15.69)	14.39	
SiO[d]	7σ	11.93	7.59(4.02)	11.61	11.61
	2π	12.90	8.22(12.24)	12.29	12.19
	6σ	16.63	10.83(14.84)	14.80	14.80
AAD(val)		0.95	4.05(0.03)	0.03	
	5σ	34.41	23.59(27.61)	28.01	
	1π	116.22	95.82(99.84)	101.62	
	4σ	116.20	95.61(99.63)	101.96	
	3σ	167.88	138.95(142.97)	145.51	
	2σ	558.69	510.48(514.50)	518.75	
	1σ	1872.70	1783.13(1787.15)	1802.16	
N_2[b,c,e]	$3\sigma_g$	17.27	10.39(5.19)	15.57	15.58
	$1\pi_u$	16.72	11.72(16.91)	16.68	16.93
	$2\sigma_u$	21.21	13.60(18.79)	18.77	18.75
AAD(val)		1.45	5.21(0.02)	0.09	
	$2\sigma_g$	40.04	28.36(33.55)	33.69	37.3
	$1\sigma_u$	426.67	383.67(388.86)	389.72	409.98
	$1\sigma_g$	426.76	383.70(388.89)	389.76	409.98
AAD(inner)		12.07	20.51(15.32)	14.70	
P_2[f]	$2\pi_u$	10.11	7.21(3.44)	10.65	10.65
	$5\sigma_g$	11.17	7.34(10.78)	10.91	10.84
AAD(val)		0.43	3.47(0.03)	0.04	
	$4\sigma_u$	16.54	11.65(15.09)	14.95	
	$4\sigma_g$	24.60	17.09(20.53)	20.53	
	$1\pi_g$	147.21	124.09(127.53)	129.64	
	$1\pi_u$	147.21	124.24(127.68)	129.65	
	$3\sigma_u$	147.20	124.25(127.69)	129.93	
	$3\sigma_g$	147.26	124.25(127.69)	129.98	
	$2\sigma_u$	204.59	172.68(176.12)	178.42	
	$2\sigma_g$	204.61	172.69(176.13)	178.43	
	$1\sigma_u$	2176.23	2079.42(2082.86)	2099.33	
	$1\sigma_g$	2176.23	2079.42(2082.86)	2099.33	
HF[b,g,h]	1π	17.69	9.75(6.44)	16.18	16.19
	3σ	20.92	13.61(20.04)	19.90	19.9
AAD(val)		1.26	6.51(0.07)	0.00	
	2σ	43.58	30.18(36.62)	36.77	39.7
	1σ	715.53	660.44(666.88)	668.33	694.23
AAD(inner)		12.59	21.65(15.21)	14.41	
HCl[l]	2π	12.97	8.13(4.64)	12.77	12.77
	5σ	17.04	11.90(16.53)	16.53	16.6
	4σ	30.41	21.22(25.86)	25.82	25.8
AAD(val)		1.75	4.68(0.04)	0.03	
	1π	218.77	190.98(195.62)	199.59	
	3σ	218.84	191.27(195.91)	199.79	
	2σ	287.75	250.44(255.08)	259.80	
	1σ	2853.04	2742.09(2746.73)	2771.13	
H_2O[b,c,d]	$1b_1$	13.85	7.32(5.3)	12.62	12.62
	$3a_1$	15.89	9.46(14.76)	14.73	14.74
	$1b_2$	19.35	13.19(18.49)	18.33	18.55
AAD(val)		1.06	5.34(0.04)	0.08	
	$2a_1$	36.67	25.36(30.66)	30.72	32.2
	$1a_1$	559.65	510.81(516.11)	517.48	539.90
AAD(inner)		12.11	17.96(12.66)	11.95	
HCN[k]	1π	13.49	9.10(4.51)	13.61	13.61

TABLE I. (*Continued*.)

	MO	HF	GGA-BP	KS	Expt.
	5σ	15.87	9.28(13.79)	14.09	14.01
	4σ	22.17	15.29(19.80)	19.95	19.86
AAD(val)		1.43	4.60(0.05)	0.06	
	3σ	33.65	23.14(27.65)	27.96	
	2σ	307.30	270.90(275.40)	276.97	
	1σ	424.49	381.39(386.10)	387.79	
FCN[l]	2π	13.68	8.83(4.82)	13.65	13.65
	7σ	16.38	9.68(14.50)	14.72	14.56
	1π	22.16	14.02(18.84)	19.74	19.3
	6σ	25.31	17.43(22.25)	22.83	22.6
AAD(val)		1.85	5.02(0.22)	0.21	
	5σ	34.26	23.59(28.41)	28.68	
	4σ	48.07	34.29(39.11)	40.19	
	3σ	310.20	273.28(278.10)	279.43	
	2σ	424.79	381.85(386.67)	387.88	
	1σ	719.44	664.26(669.08)	670.74	

[a]Reference 42.
[b]Reference 43.
[c]Reference 44.
[d]Reference 45.
[e]Reference 46.
[f]Reference 47.
[g]Reference 48.
[h]Reference 49.
[i]Reference 50.
[j]Reference 51.
[k]Reference 52.
[l]Reference 53.

III. ϵ_i OF ACCURATE KS POTENTIALS VERSUS HF ϵ_i AND EXPERIMENTAL VIPs

The orbital energies ϵ_i can be obtained with KS potentials constructed from highly accurate *ab initio* densities. In our previous publications the KS solutions have been produced for molecules of the elements of the first and second periods.[8,18–20] In this paper the KS energies ϵ_i are obtained for the closed-shell diatomic molecules SiO, P_2, and HCl of the elements Si, P, Cl of the third row. Table I presents these ϵ_i together with those for their second-row analogs CO, N_2, and HF obtained at the experimental equilibrium geometry. In addition, ϵ_i for the triatomic molecules H_2O, HCN, and FCN are calculated and they are also presented in Table I. They are compared with the experimental valence VIPs I_i determined with He(I) UV photoelectron spectroscopy (i.e., $I_i<21.2$ eV) and, in some cases, with the experimental VIPs for the deep valence and core levels. The comparison is also made with ϵ_i calculated with the Hartree–Fock (HF) method as well as with the potential of the standard DFT generalized gradient approximation (GGA), the combination BP of the exchange functional of Becke (B88) (Ref. 21) and the correlation functional of Perdew (P86).[22]

The iterative local updating scheme of van Leeuwen and Baerends (LB) (Ref. 23) has been used to get the KS solution from the *ab initio* density. The molecular KS xc potential v_{xc} is constructed in the basis of the Gaussian functions. The correct Coulombic asymptotics $-1/r$ together with the requirement, that the HOMO orbital energy ϵ_H should be close to $-I_H$, is imposed on v_{xc} within the LB scheme, as was described in Refs. 8 and 24. The *ab initio* configuration interaction (CI) calculations have been performed by means of the ATMOL package.[25] The construction of the KS solution has been performed with a Gaussian orbital density functional code[12,26] based on the ATMOL package. For the second-row elements the quadruple-zeta correlation-consistent polarized core-valence (aug-cc-pCVQZ) basis sets[27] of contracted Gaussian functions have been used with all *f*-, *g*-, and the most diffuse *d*-functions excluded. For CO, HF, and H_2O the basis sets differ from those used in our Ref. 8, so that the corresponding ϵ_i are slightly different. For H and the third-row elements similar quadruple-zeta correlation-consistent polarized valence (aug-cc-pVQZ) basis sets[28,29] without *f*-, *g*-, and the most diffuse *d*-functions have been used.

The KS orbital energies $-\epsilon_i$ closely match the experimental VIPs I_i for the valence levels (see Table I). The average (over all considered molecules) deviation of valence $-\epsilon_i$ is only 0.08 eV. In particular, for the HF molecule not only the first, but also the second VIP practically coincides with $-\epsilon_i$. For molecules of the third-row elements a typical $-\epsilon_i$ deviation Δ appears to be even smaller, than that for molecules of the second-row elements. For example, for SiO and HCl Δ is only 0.03 eV. On the other hand, the largest $\Delta=0.21$ eV is found for FCN. The KS orbital energies reproduce the trend of the experimental VIPs, namely, the valence levels ϵ_i of the third-row-element molecules SiO, P_2, and HCl are higher than the corresponding levels of their second-row-element analogues CO, N_2, and HF.

The Hartree–Fock Koopmans theorem produces, on the average, an order of magnitude worse estimate of valence VIPs (see Table I). The average (over all considered molecules) deviation for $-\epsilon_i^{HF}$ amounts to 1.27 eV, the smallest is $\Delta=0.43$ eV for P_2, while the largest is $\Delta=1.85$ eV for FCN. As a rule, Koopmans theorem considerably overestimates VIPs, due to the neglect of electron relaxation in the cationic states. Note, that for the HF HOMOs of the third-row-element molecules SiO, P_2, HCl and larger molecules HCN, FCN this lack of relaxation seems to be compensated with the neglect of electron Coulomb correlation in the HF method. Due to this, $-\epsilon_H^{HF}$ for SiO and HCl are only somewhat higher than I_H, for FCN these quantities practically

coincide, while for P_2 and HCN $-\epsilon_H^{HF}$ are even smaller than I_H. Another exception is $-\epsilon_i^{HF}$ for the $1\pi_u$ MO of N_2, which is smaller than the corresponding I_i, because of the wrong ordering of ionizations, which Koopmans theorem provides for N_2 (see Table I).

As has been already mentioned in Ref. 8, the agreement between $-\epsilon_i$ and I_i is less precise for the lower valence and core levels (see the data in Table I for CO, N_2, HF, H_2O), with the absolute $-\epsilon_i$ deviation increasing with the depth of the level. In this case the HF orbital energies ϵ_i^{HF} are consistently lower than the KS ϵ_i, so that Koopmans theorem consistently overestimates VIPs of the deep valence and core levels, while its KS analog underestimates them. It is interesting to note, that for these levels a typical $-\epsilon_i^{HF}$ deviation is always close to 12 eV, while a typical $-\epsilon_i$ deviation is close to 14.5 eV for CO, N_2, HF, and only for H_2O it is 11.95 eV, which is somewhat less than the $-\epsilon_i^{HF}$ deviation of 12.11 eV.

The BP column of Table I displays, at first glance, just the well-known feature of the GGA potentials, namely, the systematic underestimation (on absolute value) of the KS orbital energies. BP greatly underestimates $-\epsilon_i$ and I_i in all cases, with the average errors (with respect to I_i) ranging from 3.44 eV for P_2 to 6.44 eV for HF. However, a closer look at these errors reveals, how remarkably systematic they are for a particular molecule. For each molecule we present in the parentheses for the HOMO the sum $(\epsilon_H^{BP}+I_H)$, and for the other orbitals the energies shifted downward by this sum, as well as their average error (deviation from VIP). The surprising conclusion is, that the $(\epsilon_H^{BP}+I_H)$-shifted BP orbital energies reproduce the valence VIPs remarkably well (see Table I). The corresponding Δ varies from 0.02 eV for N_2 to 0.25 eV for CO, so that the average error (over all considered molecules) of 0.09 eV is practically identical to the 0.08 eV average error for the KS orbitals. For the lower valence and core levels (see the data in Table I for CO, N_2, HF, H_2O) the BP Δ values are by 0.6–1.3 eV larger than the KS ones. Thus, judging from the calculated orbital energies, the $(\epsilon_H^{BP}+I_H)$-shifted BP xc potential is close to the accurate KS one, especially in the valence region. Therefore, in spite of the well-known deficiency of the long-range asymptotics of the GGA potentials, GGA-BP may reproduce rather accurately the form of the KS potential in the bulk region.

The results of the calculations presented in this section provide further support for the interpretation of the KS orbital energies $-\epsilon_i$ as approximate relaxed VIPs [Eq. (1.8)]. In the next section individual components of the $\epsilon-I$ relations will be evaluated and the conditions of the type (4.13) will be analyzed in order to get a theoretical understanding of the correspondence between $-\epsilon_i$ and I_i established in this section.

IV. STRUCTURE OF $\epsilon-I$ RELATIONS AND NUMERICAL CONFIRMATION FOR H_2

In view of the important role of Dyson orbitals in the $\epsilon-I$ relations, we first make a few comments on the Dyson orbitals in relation to the theory of photoionization. Against that background the matrices **M** and **P** will then be discussed.

When the Hartree–Fock determinant is a good zero-order approximation of the wave function, and if there would be no electron relaxation after an orbital ionization, the Dyson orbital of that ionization would be practically identical to the Hartree–Fock orbital. The same reasoning holds when one takes the Kohn–Sham orbitals as one-particle basis (which are quite close to Hartree–Fock orbitals anyway[30]). Of course correlation effects in the ground state, and relaxation plus correlation effects in the ionized state, leading to admixture of substituted determinants, will cause deviation from precise equality between Dyson orbitals and Hartree–Fock or Kohn–Sham orbitals. Notably, the norms of the Dyson orbitals will start to deviate from 1. Note, that the d_i, defined in Eq. (1.2), are nonorthogonal, non-normal, and generally linearly dependent orbitals. The norms

$$n_i=\int |d_i(\mathbf{r}_1)|^2 d\mathbf{r}_1, \tag{4.1}$$

which obey the sum rule

$$\sum_i^{\infty} n_i = N/2 \tag{4.2}$$

are called *spectroscopic factors* and are related to the intensity of the corresponding ion state in the photoelectron spectrum. As we will see, typically—as, for instance, for the molecules investigated in the previous section—the overlap of the *normalized* Dyson orbital of a primary ionization with the corresponding Kohn–Sham orbital is very close to 1 (>0.999). The norms of these Dyson orbitals corresponding to primary ion states, typically differ less than 10% from 1. As can be seen from Eq. (1.2), these conditions will arise when the independent particle picture is a good approximation, in the sense that the ground state wave function is well approximated by a single determinant of Kohn–Sham orbitals, and when the Koopmans or frozen-orbital approximation would be reasonable for the primary ion state. These statements can be made for Hartree–Fock as well as for Kohn–Sham orbitals, the overlaps of the normalized primary Dyson orbitals with the occupied Hartree–Fock orbitals are as close to 1 as they are for the occupied Kohn–Sham orbitals. So we cannot conclude that Kohn–Sham orbitals are closer to Dyson orbitals than to Hartree–Fock orbitals.

There are many more ion states than the primary ones. Each is characterized by a Dyson orbital $d_c\,(c>H)$. These Dyson orbitals have in general quite small norms, and the intensity in the photoelectron spectrum is negligible. It occasionally happens that the norm of such a Dyson orbital is non-negligible, and the intensity in the photoelectron spectrum (the ''pole strength'' of the ionization) is then significant (usually such peaks in the photoelectron spectrum occur as satellites to the large intensity peaks of the primary ionizations).[31] We point to two situations where such behavior can occur. Suppose that electron relaxation upon a particular orbital ionization, from ϕ_i say, is described by admix-

ing to the frozen-orbital determinant describing the orbital-ionization, a certain one-electron excitation $\phi_j \rightarrow \phi_a$. This may for instance happen when the orbital ϕ_i is localized on the left atom of a diatomic, and ϕ_j is a bonding orbital and ϕ_a is an antibonding orbital. Then the $\phi_j \rightarrow \phi_a$ excitation leads to partial replacement of the density corresponding to a doubly occupied ϕ_j orbital by a density $|\phi_j + \phi_a|^2$, which is localized on the left atom. This is the expected relaxation of electron density, which moves screening charge towards the ionized atom. There is also a higher lying ion state which is the $\phi_j \rightarrow \phi_a$ excited state (''shake-up'') of the primary ion state $(\phi_i)^{-1}$. This ion state will now have, if only for orthogonality reasons, some admixture of the determinant with only the single $(\phi_i)^{-1}$ ionization (the frozen orbital determinant for the primary ionization). In the overlap Eq. (1.2) this singly ionized determinant appearing in the CI expansion of the shake-up ion state will yield, from the overlap with the leading fully occupied determinant in the neutral ground state wave function, the orbital ϕ_i as major contribution to the Dyson orbital. It will however be multiplied with the relatively small mixing coefficient of the primary ionization determinant in the shake-up wave function, hence the norm of this Dyson orbital will not be close to 1 but will be small. The corresponding intensity in the photoelectron spectrum of this ''shake-up satellite to $(\phi_i)^{-1}$'' will be much smaller than that of the primary ionization, but not negligible. Note that in this case the satellite is an excitation (''shake-up'') of just the primary ionization that is responsible for the main peak. A second case where intensity of satellite peaks appears is when an ion state that contains an excitation in addition to a (primary) ionization, becomes accidentally near-degenerate with a different primary ion state. The near-degeneracy may lead to mixing, and in that case the admixing of that primary ion state causes the Dyson orbital to be like the ionized orbital of that primary ion state, and the different-from-zero norm leads to intensity of the shake-up ion state. In this case the shake-up ion state ''steals'' intensity from the different primary ion state and appears—on account of the initial near-degeneracy—as a satellite to that primary ion state. Of course, much more intricate CI mixings will occur in many cases, and we have noticed many Dyson orbitals which (after normalization) could not be identified with a single occupied Kohn–Sham orbital. However, we do find in our present molecules a very large overlap of the normalized Dyson amplitude of the important satellites—those with nonnegligible intensity—with a single occupied Kohn–Sham orbital. In that case we can unambiguously define the set $\Omega_s(i)$ of satellites to the primary ion state $(\phi_i)^{-1}$, in the sense that their Dyson orbitals have nonnegligible norm and have, after normalization, large overlap with ϕ_i.

Let us consider the structure of the matrices **P** and $\mathbf{M}^{-1}\mathbf{P}$ against this background. As shown below we collect in the first H columns of **P** the weighted (with ρ^{-1}) overlaps of ϕ_i^2 with dj^2, and in the remaining columns those with the Dyson orbitals of the shake-up ionizations [see Eq. (1.7)]. When the ''normalized'' Dyson orbitals $n_i^{-1/2} d_i$ of the primary ionizations are close to the occupied Kohn–Sham orbitals, we can substitute $d_i = n_i^{1/2}\phi_i$ in the leading $H \times H$ block of **P** and obtain that each

Structure of matrix **P**

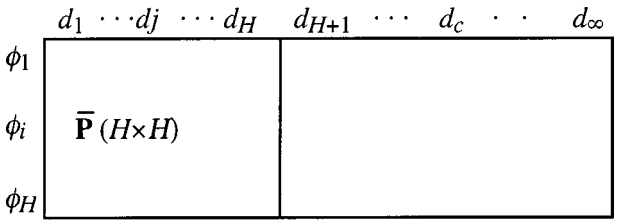

column j of this part of the **P** matrix (let us denote it as $\bar{\mathbf{P}}$) is multiplied by the corresponding n_j, i.e., $\mathbf{P} \approx \mathbf{MN}$ if **N** is diagonal, $N_{ij} = n_i \delta_{ij}$. So $\mathbf{M}^{-1}\bar{\mathbf{P}} \approx \mathbf{N}$, a diagonal matrix with the pole strengths of the primary ionizations n_i as the diagonal elements. Similarly, if $n_c^{-1/2} d_c$ of a satellite is close to an occupied KS orbital, ϕ_i say, the corresponding column of the **P** matrix becomes a weighted column of the row, $(\mathbf{M}^{-1}\mathbf{P})_{jc} \approx \delta_{ji} n_c$. This entry indicates the strength of the satellite,

Approximate structure of matrix $\mathbf{M}^{-1}\mathbf{P}$

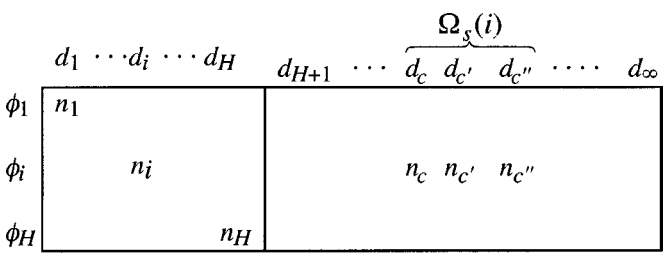

the **M** matrix, $P_{jc} \approx n_c M_{ji}$. The corresponding column of $\mathbf{M}^{-1}\mathbf{P}$, the Dyson orbital of which belongs to an ion state that is a satellite to the primary ionization from ϕ_i, will then only have an entry (n_c) at the i-? With this, the $\epsilon - I$ relations (1.7) in their simplified form (2.24) assume the form,

$$\epsilon_i \approx -n_i I_i - \sum_{c \in \Omega_s(i)} n_c I_c - \sum_{c \notin \Omega_s(i)} (\mathbf{M}^{-1}\mathbf{P})_{ic} I_c + w_i . \tag{4.3}$$

The first term in the r.h.s. of Eq. (4.3) is the contribution to ϵ_i from the primary ionization, the second term displays the satellite structure, the third term collects contributions from other ionizations, and the fourth term is the response ''step.'' For outer valence orbitals there is negligible or no satellite structure, so the pole strengths n_i of the primary ionizations are close to 1, while the last three terms are expected to be much smaller than the first one. This leads to the Koopmans interpretation Eq. (1.8) of the $\epsilon - I$ relations (1.7), $\epsilon_i \approx -I_i$. More specifically, by writing Eq. (4.3) in the form,

TABLE II. Components (eV) of the $\epsilon - I$ relations for H_2.

H_2	ϵ_H	I_H(calc.)	ϵ_H^{resp}	$\bar{n}_H$	S_{HH}	Σ'(calc.)	Σ'(estim.)
1σ	−16.44	16.44	1.25	0.953	0.99997	2.02	2.02

$$\epsilon_i \approx -I_i + (1-n_i)I_i - \sum_{c\in\Omega_s(i)} n_c I_c - \sum_{c\notin\Omega_s(i)} (\mathbf{M}^{-1}\mathbf{P})_{ic} I_c + w_i , \tag{4.4}$$

we note that the last four terms on the right-hand side of Eq. (4.4) should add up to zero in order to make the relation $\epsilon_i = -I_i$ hold. For upper valence ionizations, where the satellite structure is very weak (i.e., $n_i \approx 1$, $n_c \approx 0$) and the KLI constant very small, $w_i \approx 0$, we might expect this to happen. However, we have already indicated in Ref. 8 that the relation,

$$(1-n_i)I_i - \sum_{c\in\Omega_s(i)} n_c I_c - \sum_{c\notin\Omega_s(i)} (\mathbf{M}^{-1}\mathbf{P})_{ic} I_c + w_i \approx 0 \tag{4.5}$$

may actually depend on cancellation of these terms rather than them being individually very close to zero. A numerical

TABLE III. Components (eV) of the $\epsilon - I$ relations for CO, HF, H_2O, and HCN.

CO	5σ	1π	4σ	3σ	2σ	1σ
I_i(calc.)	14.23	17.08	20.25	36.27	⋯	⋯
				(37.35,40.12,40.35)		
ϵ_i^{resp}	4.30	6.29	6.59	7.06	28.01	39.12
$(M^{-1}\epsilon^{\text{resp}})_i$	1.83	2.75	5.11	9.07	30.97	45.16
$(M^{-1}P)_{ii}$	0.945	0.938	0.898	0.365	⋯	⋯
				(0.198,0.159,0.092)		
n_i	0.935	0.929	0.900	0.344	⋯	⋯
				(0.177,0.083,0.171)		
S_{ii}	0.9997	0.9997	0.9996	0.997	⋯	⋯
				(0.961,0.990,0.982)		
Σ'(calc.)	2.10	1.42	1.35	20.83	⋯	⋯
Σ'(estim.)	2.60	3.84	6.77	29.79	⋯	⋯
HCN	1π	5σ	4σ	3σ	2σ	1σ
I_i(calc.)	13.59	14.37	21.05	30.88	⋯	⋯
				(35.84)		
ϵ_i^{resp}	5.07	5.49	4.15	6.13	28.43	33.96
$(M^{-1}\epsilon^{\text{resp}})_i$	1.64	3.64	3.21	8.06	31.67	38.45
$(M^{-1}P)_{ii}$	0.954	0.891	0.931	0.538	⋯	⋯
				(0.123)		
n_i	0.939	0.912	0.923	0.567	⋯	⋯
				(0.099)		
S_{ii}	0.9995	0.9990	0.9998	0.9985	⋯	⋯
				(0.961)		
Σ'(calc.)	1.11	2.07	0.83	10.87	⋯	⋯
Σ'(estim.)	2.27	5.17	4.67	19.41	⋯	⋯

H_2O	$1b_1$	$3a_1$	$1b_2$	$2a_1$	$1a_1$
I_i(calc)	12.74	14.96	18.94	32.65	⋯
				(34.22)	
ϵ_i^{resp}	6.21	6.03	5.66	6.27	38.94
$(M^{-1}\epsilon^{\text{resp}})_i$	2.66	3.33	1.55	10.61	44.98
$(M^{-1}P)_{ii}$	0.920	0.906	0.934	0.520	⋯
				(0.291)	
n_i	0.922	0.923	0.933	0.504	⋯
				(0.304)	
S_{ii}	0.9997	0.9994	0.99990	0.9994	⋯
				(0.9998)	
Σ'(calc.)	2.51	1.23	1.85	12.50	⋯
Σ'(estim.)	3.64	4.71	2.55	24.59	⋯

HF	1π	3σ	2σ	1σ
I_i(calc.)	16.26	20.10	39.38	⋯
			(42.84)	
ϵ_i^{resp}	7.16	6.61	7.01	43.05
$(M^{-1}\epsilon^{\text{resp}})_i$	3.34	2.75	10.91	50.65
$(M^{-1}P)_{ii}$	0.939	0.869	0.539	⋯
			(0.111)	
n_i	0.924	0.931	0.733	⋯
			(0.140)	
S_{ii}	0.9998	0.996	0.994	⋯
			(0.996)	
Σ'(calc.)	3.68	4.18	11.85	⋯
Σ'(estim.)	4.32	5.36	26.21	⋯

investigation of these relations will be given in this section (for H_2) and the next section (for some other prototype molecules).

Tables II and III present individual components of the $\epsilon-I$ relations (1.7) calculated for the closed-shell molecules H_2, CO, HF, H_2O, HCN. The Dyson orbitals have been obtained with the MELD package,[32] in particular, the program CISTAR of this package has been used to generate the wave functions ${\Psi_0}^{N00}$, ${\Psi_0}^{(N-1)1/21/2}$ and to calculate the ionization energies, and the program PES has been used for the subsequent calculation of d_i according to Eq. (1.2). For each irreducible representation of the molecular symmetry group MELD allows us to calculate up to 50 Dyson orbitals and the highest possible symmetry group is D_{2h}. The matrices $\mathbf{M}$, $\mathbf{P}$, $\boldsymbol{\epsilon}^{\text{resp}}$ and their combinations $\mathbf{M}^{-1}\mathbf{P}$, $\mathbf{M}^{-1}\mathbf{PI}$, and $\mathbf{M}^{-1}\boldsymbol{\epsilon}^{\text{resp}}$ in Eq. (1.7) have been calculated with the abovementioned Gaussian orbital density functional code[12,26] based on the ATMOL package.[25] In particular, the response potential v_{resp} has been calculated on a numerical grid by the direct subtraction (3.9) of the potentials $v_{c,\text{kin}}$ and $v_{\text{xc}}^{\text{hole}}$ from the constructed KS potential v_{xc} with subsequent numerical integration to get the matrix elements ϵ_i^{resp}. To do this, the potential $v_{\text{xc}}^{\text{hole}}$ of Eq. (2.19) has been constructed from the second-order density matrix with the codes.[12,26] The MELD calculations have been performed in the same basis sets as the ATMOL ones described in the previous section. The same basis sets have been used for N and $(N-1)$ electron systems, which is required to calculate the Dyson orbitals with the PES program.

Within these basis sets, the summation over the Dyson orbitals, which is required in order to get the matrix $\mathbf{M}^{-1}\mathbf{PI}$, certainly surpasses (even for small molecules) the limitations of MELD. The problem, however, is greatly simplified for two-electron systems. In this case the $(N-1)$ electron wave functions turn into the Hartree–Fock orbitals of a single-electron system, so that calculation of all Dyson orbitals in the chosen basis becomes feasible. Thus, one can use benchmark two-electron calculations to check numerically the validity of the $\epsilon-I$ relations. For a closed-shell two-electron system we have just one occupied KS orbital ϕ_H. Since $2(\phi_H)^2=\rho$, $M_{11}=1$, and all matrix elements $(\mathbf{M}^{-1}\mathbf{P})_{H,i}$ turn exactly to the pole strengths n_i. Then, the $\epsilon-I$ relations (1.7) are reduced to a single equation,

$$\epsilon_H=-\sum_i n_i I_i+\epsilon_H^{\text{resp}}, \tag{4.6}$$

$$\sum_i^{\infty} n_i=1. \tag{4.7}$$

Remarkably, the first term in the r.h.s. of Eq. (4.6) has an ''average spectroscopic'' structure in the sense, that individual ionizations appear in it with weights n_i that correspond to the intensities in the photoelectron spectrum of H_2. Taking into account the exact property $\epsilon_H=-I_H$ of the HOMO, we can rewrite Eq. (4.6) in the form,

$$(1-n_H)I_H-\sum_i{}' n_i I_i+\epsilon_H^{\text{resp}}=0, \tag{4.8}$$

where the prime on the summation indicates omission of the $i=H$ term.

Table II presents the ingredients of the equality (4.8) as well as the overlap S_{HH},

$$S_{HH}=\frac{1}{\sqrt{n_H}}\int \phi_H(\mathbf{r})d_H(\mathbf{r})d\mathbf{r} \tag{4.9}$$

between the KS orbital ϕ_H and the normalized Dyson orbital $n_H^{-1/2}d_H$ of the primary ionization calculated for the H_2 molecule. This calculation has been performed in the 6-zeta aug-cc-pV6Z basis[28] without *f*-, *g*-, and *h*-functions. The VIP of 16.44 eV calculated with the full CI in this large basis is taken as I_H. Though more than an order of magnitude smaller than I_H, the calculated contribution $\epsilon_H^{\text{resp}}=1.25$ eV of the response potential is still an appreciable quantity.[33]

Judging from the overlap integral $S_{HH}=0.99997$, the form of the Dyson orbital of the primary ionization d_H is very close to that of the σ_g KS orbital ϕ_H. Even though the d_H after normalization is very similar to ϕ_H, its norm clearly deviates from 1, with the corresponding pole strength $n_H=0.953$. With this, the first term in the r.h.s. of Eq. (4.8) amounts to 0.77 eV which, together with ϵ_H^{resp}, yields 2.02 eV. As follows from Eq. (4.8), this quantity should be exactly compensated with the contributions from higher ionizations, in order that the $\epsilon-I$ relations (1.7) would provide the exact property $\epsilon_H=-I_H$ for the HOMO of H_2. Thus, the value of 2.02 eV of the primed sum estimated from I_H, ϵ_H^{resp}, and n_H is placed in Table II in the entry Σ'(estim).

The largest pole strength $n_2=0.024$ in the primed sum in Eq. (4.8) belongs to the ionization with VIP $I_2=40.62$ eV to the $2\sigma_g$ state of the cation H_2^+. The next two largest contributions come from higher ionizations with $I_4=46.23$ eV and $I_6=50.39$ eV, however, the corresponding pole strengths $n_4=0.0025$ and $n_6=0.0024$ are an order of magnitude smaller than n_2. The summed contributions of these satellites to the sum $\Sigma_{i>1}-n_iI_i$ is 1.21 eV, which amounts to 60% of the required 2.02 eV. The rest of the sum is scattered over many other ionizations.

Remarkably, the direct calculation of the total sum over higher ionizations (with all ionizations within the basis set included) yields just 2.02 eV [the entry Σ'(calc.) in Table II], so that these ionizations provide the required compensation of $\Sigma_{i>1}-n_iI_i$ to $(1-n_H)I_H+\epsilon_H^{\text{resp}}$ to within 0.01 eV. Apparently the completeness which requires that summation is extended over the continuum of ion states (with the second electron also ionized) is approximated to this level of precision by our discrete sum over the ion states described in the finite basis. This means, that in the case of H_2 the $\epsilon-I$ relations agree perfectly with the well established condition $\epsilon_H=-I_H$. Thus, the present benchmark calculations for H_2 provide a numerical confirmation for the $\epsilon-I$ relations (1.7).

We note that the $\epsilon_H=-I_H$ relation in this case does not at all arise from smallness of the individual terms in (4.8). We will investigate in the next section whether in general the remarkable correspondence between KS orbital energies and VIPs arises from cancellation in the terms of Eq. (4.5) rather than from them individually being negligible.

V. EVALUATION OF INDIVIDUAL COMPONENTS OF THE $\epsilon - I$ RELATIONS FOR CO, HF, H_2O, AND HCN

Calculation of the components of the $\epsilon - I$ relations for CO, HF, H_2O, and HCN produces a coherent picture for all molecules considered (see Table III). In all cases the Dyson orbitals of the primary ionizations from the core levels are not among the first 50 d_i of the corresponding irreducible representation allowed by MELD. Thus, the related entries in Table III are empty. Table III presents the calculated valence VIPs I_i of primary ionizations and, in the case of deep valence levels, also (in parentheses) the VIPs of the most important satellites. In most cases, the calculated VIPs are larger than the experimental ones (compare Tables I and III), though the quality of the calculated VIPs is reasonable. A possible reason for this overestimation is the use of the same basis sets for neutral and cationic systems. The basis is optimized for the neutral molecule and may be less well adapted for the ion. Also the correlation treatment of the ion is possibly less effective.

The only data in Table III displayed for both core and valence levels are the KS orbital matrix elements $\epsilon_i^{\mathrm{resp}}$ of the response potential and the matrix elements $(\mathbf{M}^{-1}\boldsymbol{\epsilon}^{\mathrm{resp}})_i$, which are components of the $\epsilon - I$ relations. These have been calculated by the ATMOL based DFT code as was described above. Both $\epsilon_i^{\mathrm{resp}}$ and $(\mathbf{M}^{-1}\boldsymbol{\epsilon}^{\mathrm{resp}})_i$ represent the characteristic step structure of v_{resp}, with lower values for valence levels and higher values for core levels. Note, that the $\epsilon_i^{\mathrm{resp}}$ values for deep valence levels are not much distinguished from those for outer valence levels. In particular, for H_2O the $\epsilon_i^{\mathrm{resp}}$ value of 6.27 eV for the deep valence KS level $2a_1$ is very close to that of 6.21 eV for the HOMO $1b_1$, while for HF the $\epsilon_i^{\mathrm{resp}}$ value 7.01 eV for the 2σMO is even lower than that of 7.16 eV for the HOMO 1π. Thus, for each molecule all the valence $\epsilon_i^{\mathrm{resp}}$ values form kind of a ''plateau,'' above which stand the core $\epsilon_i^{\mathrm{resp}}$ values (see Table III).

Remarkably, the action of the matrix $\mathbf{M}^{-1}$ makes the calculated $(\mathbf{M}^{-1}\boldsymbol{\epsilon}^{\mathrm{resp}})_i$ values for outer valence levels consistently smaller compared to the corresponding $\epsilon_i^{\mathrm{resp}}$ and it raises $(\mathbf{M}^{-1}\boldsymbol{\epsilon}^{\mathrm{resp}})_i$ for deep valence levels. As a result, only the outer valence $(\mathbf{M}^{-1}\boldsymbol{\epsilon}^{\mathrm{resp}})_i$ values form a ''plateau,'' with the deep valence $(\mathbf{M}^{-1}\boldsymbol{\epsilon}^{\mathrm{resp}})_i$ standing appreciably higher and the core $(\mathbf{M}^{-1}\boldsymbol{\epsilon}^{\mathrm{resp}})_i$ still higher (see Table III). $(\mathbf{M}^{-1}\boldsymbol{\epsilon}^{\mathrm{resp}})_i$ do not necessarily follow the order of the orbital energies $-\epsilon_i$. For example, for both H_2O and HF the smallest $(\mathbf{M}^{-1}\boldsymbol{\epsilon}^{\mathrm{resp}})_i$ values correspond not to the HOMOs, but to the $1b_2$ and 3σMO, respectively. Though much smaller than VIPs I_i, the elements $(\mathbf{M}^{-1}\boldsymbol{\epsilon}^{\mathrm{resp}})_i$ are appreciable even for outer MOs, ranging in this case from 1.55 eV for the $1b_2$ MO of H_2O to 5.11 eV for the 4σMO of CO. Thus, in the context of $\epsilon - I$ relations, the close correspondence between outer valence $-\epsilon_i$ and I_i established in Sec. III has to be achieved through the compensation of $(\mathbf{M}^{-1}\boldsymbol{\epsilon}^{\mathrm{resp}})_i$ with the contributions $\Sigma_k'(\mathbf{M}^{-1}\mathbf{P})_{ik}I_k$ from other ionizations, as happens for the benchmark case of H_2 considered in the previous section.

We proceed with the discussion of the calculated Dyson orbitals d_i and the ingredients of Eqs. (1.7), which include d_i. For all presented orbitals d_i of the primary ionizations their overlap integrals S_{ii} with the KS orbitals ϕ_i are very close to 1 (after normalization of the d_i) so that, judging from this criterion, the form of d_i is close to that of ϕ_i. This confirms the anticipation of Refs. 16 and 34, although we should caution that also the Hartree–Fock orbitals have similarly large overlaps with the (normalized) Dyson orbitals. It is interesting to consider cases where Hartree–Fock orbitals differ essentially from the Kohn–Sham orbitals and Dyson orbitals. In one such case (the Cu_3Cl_3 molecule) it was observed[35] that the Kohn–Sham orbitals do correspond more closely to the Dyson orbitals. This molecule exhibits the ''breakdown of Koopmans' theorem'' for transition metal complexes observed long ago by Veillard and co-workers;[36,37] the metal d electrons are more loosely bound according to the photoionization experiment, but the predominantly $3d$ Hartree–Fock levels lie below the predominantly Cl $3p$ ones. This is not a correlation effect, but it is a consequence of the tight nature of the $3d$ orbitals and the ensuing strong stabilizing effect of the (self-energy correction part) of the Hartree–Fock exchange operator for the $3d$ orbitals. The Kohn–Sham orbitals, with their single local potential for all orbitals, do not exhibit this reversal in the order of metal and ligand levels. The Dyson orbital of the $3d$ ionization also exhibits the $3d$ character and it is demonstrated nicely in Ref. 35 that it corresponds to the upper Kohn–Sham orbital (with $3d$ character), not to the upper Hartree–Fock orbital (with Cl $3p$ character). It would be interesting to extend such investigations into the nature of Kohn–Sham and Dyson orbitals to molecules with strong correlation effects.

In our molecules, there is no ambiguity in the identification of the d_i that belong to the primary ionizations. The amplitudes of the outer valence d_i (ionization energies below 22 eV) are also fairly close to that of ϕ_i, with the corresponding pole strengths n_i higher than 0.9. The n_i for ionization from 4σ MO of CO is the lowest, being precisely equal to 0.900. In contrast, the pole strength distribution for ionizations from the deep valence levels exhibits an important satellite structure. In this case, n_i of the primary ionization is considerably smaller than 1 ranging from 0.365 for the 3σ level of CO to 0.733 for the 2σ level of HF. Nevertheless, the overlap of the normalized Dyson orbital with the corresponding Kohn–Sham orbital remains close to 1 (>0.99), so the shape of the Dyson orbital remains similar to that of the KS orbital, only the amplitude is diminished in accordance with the $\sqrt{n_i}$ factor.

When n_i differs from 1 we expect strong satellites. The satellite pole strengths (n_c), which are close to or larger than 0.1 are presented in Table III in parentheses. For CO there are three such satellites for the 3σ orbital, with the pole strengths of 0.177, 0.083, and 0.171, and VIPs 37.35, 40.12, and 40.35 eV, respectively. The overlaps of the normalized Dyson orbitals $n_c^{-1/2}d_c$ with the corresponding KS orbital, 3σ, are also given in parentheses, below the overlap of the Dyson orbital of the primary ion state with the 3σ orbital. They are also very close to 1, identifying these ion states as satellites to $(3\sigma)^{-1}$. The nature of these satellites can be deduced from the ion wave functions. The first, at 37.35 eV, is a clear-cut example of the second type of satellite men-

tioned in the discussion above. The satellite ion state corresponds to $(5\sigma)^{-1}$ ionization accompanied with $\pi\rightarrow\pi^*$ excitation. The satellite at 40.12 eV is rather more mixed, it contains shake-ups to the $(5\sigma)^{-1}$ primary ionization (both $5\sigma\rightarrow\sigma^*$ and $\pi\rightarrow\pi^*$ shake-ups) and also to the $(4\sigma)^{-1}$ primary ionization ($5\sigma\rightarrow\sigma^*$ shake-up). The third satellite, at 40.35 eV, consists of shake-ups to the $(4\sigma)^{-1}$ primary ionization, this time mostly the $\pi\rightarrow\pi^*$ excitation with some admixture of $5\sigma\rightarrow\sigma^*$ excitation. In all these satellite wave functions the determinant of the $(3\sigma)^{-1}$ primary ionization has a significant coefficient, doubtless due to "near-degeneracy" mixing of the shake-up states of the $(5\sigma)^{-1}$ and $(4\sigma)^{-1}$ ionizations with the $(3\sigma)^{-1}$ primary ionization. This lends the Dyson orbitals of these ion states the 3σ shape, which in turn causes the corresponding spectroscopic factors to appear on the row of the $\mathbf{M}^{-1}\mathbf{P}$ matrix for the $\epsilon_{3\sigma}$ KS orbital energy.

It is interesting to consider the structure of the $\mathbf{M}^{-1}\mathbf{P}$ matrix in the case of CO:

Approximate structure of matrix $\mathbf{M}^{-1}\mathbf{P}$ for the Σ symmetry of CO

	$d_{5\sigma}$	$d_{4\sigma}$	$\cdots$ $d_{3\sigma}$	d_4 d_5 d_6 d_7 d_8 d_9	d_{10}	d_{11}	d_∞
$\phi_{5\sigma}$	0.945	0.006	–0.0006	0.015	0.001	0.007	
$\phi_{4\sigma}$	0.0005	0.898	–0.007	–0.016	–0.001	–0.0004	
$\phi_{3\sigma}$	0.009	0.020	0.365	0.198	0.092	0.159	

We note that the quasidiagonal structure of the leading $H\times H$ block is evident, as well as the structure of the satellite columns, which only exhibit a significant element in the row for the KS orbital to which the column's ion state is a satellite.

For other molecules just one satellite has a pole strength higher than 0.1, with the largest satellite pole strength $n_c=0.304$ being calculated for the satellite of the $2a_1$ level of H_2O with VIP $I_c=34.22$ eV, while the calculated pole strength of the primary ionization from $2a_1$ is $n_i=0.504$ with VIP $I_i=32.65$ eV. This satellite corresponds to ionization to the $(N-1)$ state $\Psi^{(N-1)1/2,1/2}$, which is a mixture of the primary electron configuration with a single hole $(1h)$ in the $2a_1$ MO with a $(2h1p)$ configuration with a double hole in the $1b_2$ MO (which represents the π-electron lone pair of O) and a single electron excited to the O–H antibonding MO). This is a shake-up of the primary $1b_2^{-1}$ ionization, with ionization from $1b_2$ accompanied with excitation $1b_2\rightarrow\sigma^*$(O–H). We are therefore again dealing with the second case we discussed in the introduction to the previous section, i.e., a shake-up state $(1b_2\rightarrow 4a_1)$ of the $1b_2^{-1}$ primary ionization steals intensity from the $2a_1^{-1}$ primary ion state with which is nearly degenerate. There is also some mixing into this ion state of a shake-up of the $3a_1^{-1}$ primary ion state, namely the $3a_1\rightarrow\sigma^*$(O–H) excitation. The large contribution in this wave function of the $2a_1^{-1}$ determinant lends the Dyson orbital its $2a_1$ shape (note the overlap of 0.9998 of the normalized Dyson orbital with the $2a_1$ Kohn–Sham orbital in Table III).

The structure of the $\mathbf{M}^{-1}\mathbf{P}$ matrix in the A_1 block of H_2O is calculated to be:

Approximate structure of matrix $\mathbf{M}^{-1}\mathbf{P}$ for the A_1 symmetry of H_2O

	d_{3a_1}	d_{2a_1}	d_3	d_4	$\cdots$	d_∞
ϕ_{3a_1}	0.906	–0.0085	–0.0039			
ϕ_{2a_1}	0.039	0.520	0.29			

Again the strongly diagonal nature of the $\overline{\mathbf{P}}(H\times H)$ matrix, with diagonal elements close to the n_{3a_1} and n_{2a_1} (cf. Table III) is evident. The calculated VIPs and pole strengths agree reasonably with the experimental estimates[38] $n_i^{\mathrm{exp}}=0.58$ and $I_i^{\mathrm{exp}}=32.2$ eV for the primary ionization and $n_c^{\mathrm{exp}}=0.18$, $I_c^{\mathrm{exp}}=35.0$ eV for the satellite. Previous calculation of H_2O in a smaller basis[31] gave $n_i=0.44$, $I_i=33.1$ eV for the primary ionization and $n_c=0.22$, $I_c=33.6$ eV for the satellite. From the comparison of these data one can see, that our calculation has produced VIPs and n_i, which are closer to experiment, while in Ref. 31 an n_c value closer to the experiment has been obtained.

So the calculated $\mathbf{M}^{-1}\mathbf{P}$ matrices have, indeed, the simple structure that was anticipated in Sec. III. They have quasidiagonal $H\times H$ blocks for primary ionizations with small off-diagonal elements and the satellite columns have the unit-vector (times n_c) like structure. Table III presents the diagonal elements $(\mathbf{M}^{-1}\mathbf{P})_{ii}$ for the primary ionizations and (in parentheses) the elements $(\mathbf{M}^{-1}\mathbf{P})_{ic}$ for major satellites. Comparison of these elements with the pole strengths shows that in all cases $(\mathbf{M}^{-1}\mathbf{P})_{ii}$ and $(\mathbf{M}^{-1}\mathbf{P})_{ic}$ are close to the corresponding n_i and n_c. The only exception is the 2σ level of HF, for which the n_i value is appreciably larger than $(\mathbf{M}^{-1}\mathbf{P})_{ii}$. Thus, indeed, the elements of the leading $H\times H$ block of $\mathbf{M}^{-1}\mathbf{P}$ can be represented with the approximate equality $(\mathbf{M}^{-1}\mathbf{P})_{ji}\approx\delta_{ji}n_i$, and for the satellite columns the approximate equality $(\mathbf{M}^{-1}\mathbf{P})_{jc}\approx\delta_{ji}n_c(c\in\Omega_s(i))$ holds true. From this follows, that for each ϵ_i the term $(\mathbf{M}^{-1}\mathbf{PI})_i$ in Eq. (1.7) can be fairly represented with the "spectroscopic average" $\Sigma_j n_j I_j$ over the primary ionization and the related satellites.

Just as was done for H_2 in the previous section, for all valence levels of the molecules considered in this section the contribution to ϵ_i of Eq. (1.7) from other (than I_i) VIPs has been calculated. As follows from Eq. (1.7), the full sum over other VIPs should be equal to the following combination of other ingredients:

$$\sum_k{}'(\mathbf{M}^{-1}\mathbf{P})_{ik}I_k=-(\mathbf{M}^{-1}\mathbf{P})_{ii}I_i-\epsilon_i+(\mathbf{M}^{-1}\boldsymbol{\epsilon}^{\mathrm{resp}})_i. \tag{5.1}$$

In Table III, the sum of the l.h.s. of Eq. (5.1) is calculated for each level over the first 50 terms (the infinite sum has to be restricted to a finite number of terms, and 50 corresponds to the abovementioned program limitation). The result is placed in the entry Σ'(calc.), while the combination in the r.h.s. of Eq. (5.1) with the KS orbital energy ϵ_i and the experimental VIP I_i is placed as an estimate of the primed sum in the entry Σ'(estim.). Since the quantities ϵ_i, $\epsilon_k^{\mathrm{resp}}$, and $\mathbf{M}^{-1}$ are obtained from a rather accurate KS solution, we expect Σ'(estim.) to be a reasonable estimate of the primed sum.

As one can see from Table III, Σ'(calc.) is not precisely equal to Σ'(estim.), as was the case for their H_2 analogs (see Table II). In fact, in all cases Σ'(calc.) is consistently lower than Σ'(estim.). For some levels Σ'(calc.) does agree reasonably with Σ'(estim.). For example, for the 5σ HOMO of CO Σ'(calc.) is only 0.5 eV lower than Σ'(estim.), and for the 1π HOMO of HF and $1b_2$ MO of H_2O the corresponding differences are only 0.6 and 0.7 eV, respectively. However, for other outer valence levels the differences in general amount to a few eV and for the deep valence levels these differences are about 10 eV or more. An apparent reason for this discrepancy is the restricted summation over ionizations in the primed sum Σ'(calc.). Unlike in the benchmark H_2 calculation of the previous section, the summation in Σ'(calc.) for the considered molecules is far from being complete, which is especially true for the deep valence levels. Apparently the omitted ionization channels, of which there are infinitely many (including the continuum states of the ion) contribute significantly to the total sum. Another possible reason is the limited (within the restricted CI) accuracy of the calculated VIPs I_i and Dyson orbitals d_i for higher ionizations, which might require a higher level of the correlated calculations. Nevertheless, we assume that VIPs I_i and the matrix elements $(\mathbf{M}^{-1}\mathbf{P})_{ji}$ for the orbitals d_i of the primary ionizations and major satellites are calculated with a reasonable accuracy, so that the calculations of this section provide a valuable numerical analysis of the structure of the $\epsilon-I$ relations.

VI. CONCLUSIONS

In this paper both theoretical and numerical insight has been gained into the relations between the Kohn–Sham orbital energies and relaxed vertical ionization potentials, which provide DFT and SDFT analogs of Koopmans' theorem.

Since the $\epsilon-I$ relations involve in a constructive way the Dyson orbitals, a connection has been established between the KS and Dyson orbital theories. Using the technique of the total and partial conditional probability amplitudes, the one-electron equations for the Dyson spin–orbitals and the Schrödinger equation for the square root of the total spin-density have been derived as the limiting cases of a universal equation for a partial spin-density. With this, the spin-unrestricted KS xc potential is expressed as the statistical average of individual xc potentials for the Dyson spin–orbitals, plus the correction $v_{c,\mathrm{kin},\sigma}$ due to the correlation kinetic effect, plus the correction $v_{\mathrm{resp},\sigma}$ to the energy of $(N-1)$ electrons due to the correlation with the reference electron.

Accurate KS calculations for some prototype second- and third-row closed-shell molecules have confirmed the Koopmans type interpretation of the $\epsilon-I$ relations, according to which the KS orbital energies $-\epsilon_i$ can be considered as approximate *relaxed* VIPs I_i. The valence energies $-\epsilon_i$ correspond closely to the experimental VIPs with an average deviation of only 0.08 eV. The Hartree–Fock Koopmans theorem produces, on average, more than an order worse estimate of the valence VIPs with an average deviation of 1.27 eV. The GGA-BP systematically underestimates $-\epsilon_I$, however, if the HOMO is shifted down to $-I_H$ and all the other orbitals uniformly shifted by the same amount $-(\epsilon_H^{\mathrm{BP}}+I_H)$, the BP orbital energies reproduce the valence VIPs remarkably well. This adds to the celebrated good performance of GGA for the calculation of the total energies (which is a global minimum property) also a good quality of GGA from the point of view of the form of the potential in the bulk region, which is a more sensitive criterion.

A benchmark calculation of the components of the $\epsilon-I$ relations for the H_2 molecule has provided a numerical confirmation of these relations. For the single occupied σ_g KS orbital the $\epsilon-I$ relation yields precisely the established property $\epsilon_H=-I_H$, since the sum over higher ionizations is totally compensated (within an accuracy of 0.01 eV) with the contribution $\epsilon_H^{\mathrm{resp}}$ from the response potential and the residue $(1-n_H)I_H$ of the primary ionization potential.

Calculation of the components of the $\epsilon-I$ relations for the molecules CO, HF, H_2O, and HCN has revealed the structure of these relations and the relative magnitude of their individual components. The KS and Dyson orbitals have been compared. The shape and amplitude of all outer valence Dyson orbitals of the primary ionizations are close to those of the corresponding KS orbitals. However, only the shape of the deep valence Dyson orbitals of the primary ionization resembles that of the KS orbitals, while the amplitude of the Dyson orbitals is considerably smaller and, accordingly, appreciable satellite Dyson orbitals have been found for the deep valence levels. As a result of this, the calculated $\mathbf{M}^{-1}\mathbf{P}$ matrix has a quasidiagonal $H\times H$ block for primary ionizations, $(\mathbf{M}^{-1}\mathbf{P})_{ji}\approx\delta_{ji}n_i$, and the satellite columns have the special structure $(\mathbf{M}^{-1}\mathbf{P})_{jc}\approx\delta_{ji}n_c(c\in\Omega_s(i))$. This renders for the first term in the r.h.s. of the $\epsilon-I$ relations (1.7) an interesting and physically meaningful interpretation as ''average spectroscopic structure'' due to the primary ionizations and satellites. In its turn, the second term of the r.h.s. of Eq. (1.7) exhibits for the various KS orbitals a characteristic step pattern with a ''plateau'' for the outer valence orbitals and atomic-shell steps for the deep valence and core levels.

The present theoretical and numerical results provide a basis for the understanding and interpretation of Kohn–Sham theory in terms of the molecular electronic structure and they also provide a connection with other one-electron theories. In this paper a connection has been made between the Kohn–Sham and Dyson one-electron theories. As concerns the eigenvalue spectra, the main point of the present paper, the one-electron equations for the Dyson orbitals seem to be a more natural counterpart for the KS equations than the one-electron equations for the natural orbitals (NOs).[39] Indeed, as we have established, the energies of the occupied KS orbitals are distributed just like (minus) VIPs, which are the eigenvalues of the Dyson orbitals of the primary ionizations. Compared to this, NOs have a very different distribution of the eigenvalues, with a degeneracy of all orbitals which have the same occupation.[40,41]

ACKNOWLEDGMENT

We are grateful to Professor E. R. Davidson for providing us with a copy of the MELD program package and for help with its use.

[1] W. Kohn and L. J. Sham, Phys. Rev. A **140**, 1133 (1965).
[2] W. Kohn, A. D. Becke, and R. G. Parr, J. Phys. Chem. **100**, 12974 (1996).
[3] E. J. Baerends and O. V. Gritsenko, J. Phys. Chem. A **101**, 5383 (1997).
[4] U. von Barth and L. Hedin, J. Phys. C **5**, 1629 (1972).
[5] M. M. Pant and A. K. Rajagopal, Solid State Commun. **10**, 1157 (1972).
[6] A. K. Rajagopal, Adv. Chem. Phys. **41**, 59 (1980).
[7] J. Katriel and E. R. Davidson, Proc. Natl. Acad. Sci. U.S.A. **77**, 4403 (1980).
[8] D. P. Chong, O. V. Gritsenko, and E. J. Baerends, J. Chem. Phys. **116**, 1760 (2002).
[9] O. V. Gritsenko and E. J. Baerends, J. Chem. Phys. **117**, 9154 (2002).
[10] O. V. Gritsenko, R. van Leeuwen, and E. J. Baerends, J. Chem. Phys. **101**, 8955 (1994).
[11] R. van Leeuwen, O. V. Gritsenko, and E. J. Baerends, Z. Phys. D: At., Mol. Clusters **33**, 229 (1995).
[12] M. A. Buijse, E. J. Baerends, and J. G. Snijders, Phys. Rev. A **40**, 4190 (1989).
[13] O. Gunnarsson and B. I. Lunqvist, Phys. Rev. B **13**, 4274 (1976).
[14] O. V. Gritsenko and E. J. Baerends, Phys. Rev. A **54**, 1957 (1996).
[15] O. V. Gritsenko, S. J. A. van Gisbergen, P. R. T. Schipper, and E. J. Baerends, Phys. Rev. A **62**, 012507 (2000).
[16] M. Casida, Phys. Rev. A **51**, 2005 (1995).
[17] J. B. Krieger, Y. Li, and G. J. Iafrate, Phys. Rev. A **46**, 5453 (1992).
[18] O. V. Gritsenko, R. van Leeuwen, and E. J. Baerends, J. Chem. Phys. **104**, 8535 (1996).
[19] P. R. T. Schipper, O. V. Gritsenko, and E. J. Baerends, Phys. Rev. A **57**, 1729 (1998).
[20] P. R. T. Schipper, O. V. Gritsenko, and E. J. Baerends, Theor. Chem. Acc. **99**, 329 (1998).
[21] A. Becke, Phys. Rev. A **38**, 3098 (1988).
[22] J. P. Perdew, Phys. Rev. B **33**, 8822 (1986); **34**, 7406(E) (1986).
[23] R. van Leeuwen and E. J. Baerends, Int. J. Quantum Chem. **52**, 711 (1994).
[24] P. R. T. Schipper, O. V. Gritsenko, and E. J. Baerends, Theor. Chem. Acc. **98**, 16 (1997).
[25] V. R. Saunders and J. H. van Lenthe, Mol. Phys. **48**, 923 (1983).
[26] M. A. Buijse, thesis, Vrije Universiteit, 1991.
[27] D. E. Woon and T. H. Dunning, J. Chem. Phys. **103**, 4572 (1995).
[28] T. H. Dunning, Jr., J. Chem. Phys. **90**, 1007 (1988).
[29] D. E. Woon and T. H. Dunning, J. Chem. Phys. **98**, 1358 (1993).
[30] O. V. Gritsenko, P. R. T. Schipper, and E. J. Baerends, J. Chem. Phys. **107**, 5007 (1997).
[31] A. O. Bawagan, C. E. Brion, E. R. Davidson, and D. Feller, Chem. Phys. **113**, 19 (1987).
[32] E. R. Davidson, Quantum Chemistry Program Exchange, No. 580.
[33] Note that this number was quoted in Ref. 8 erroneously as 0.98 eV, which is actually the value at $R=3.0$ bohr, cf. Ref. 12.
[34] P. Duffy, D. P. Chong, M. E. Casida, and D. R. Salahub, Phys. Rev. A **50**, 4707 (1994).
[35] P. R. Koren, F. Chen, and E. R. Davidson, Mol. Phys. **99**, 1329 (2001).
[36] J. Demuynck and A. Veillard, Theor. Chim. Acta **28**, 241 (1973).
[37] A. Veillard and J. Demuynck, in *Modern Theoretical Chemistry*, edited by H. F. Schaefer (Plenum, New York, 1977), p. 187.
[38] A. O. Bawagan, L. Y. Lee, K. T. Leung, and C. E. Brion, Chem. Phys. **99**, 367 (1985).
[39] P. O. Löwdin, Phys. Rev. **97**, 1474 (1955).
[40] T. L. Gilbert, Phys. Rev. B **12**, 2111 (1975).
[41] R. A. Donnelly and R. G. Parr, J. Chem. Phys. **69**, 4431 (1978).
[42] D. W. Turner, C. Baker, A. D. Baker, and C. R. Brundle, *Molecular Photoelectron Spectroscopy* (Wiley-Interscience, New York, 1971).
[43] G. Cavigliasso and D. P. Chong, Can. J. Chem. **77**, 24 (1999).
[44] K. Siegbahn, C. Nordling, G. Johansson, J. Hedman, P. F. Heden, K. Hamrin, U. Gelius, T. Bergmark, L. D. Werme, R. Manne, and Y. Baer, *ESCA Applied to Free Molecules* (North-Holland, Dordrecht, 1969).
[45] E. A. Colbourne, J. M. Dyke, P. F. Lee, A. Morris, and I. R. Trickle, Mol. Phys. **35**, 873 (1978).
[46] P. Baltzer, M. Larsson, L. Karlsson, B. Wannberg, and C. Göthe, Phys. Rev. A **46**, 5545 (1992).
[47] A. W. Potts, K. G. Glenn, and W. C. Price, Faraday Discuss. Chem. Soc. **54**, 65 (1972).
[48] G. Bieri, A. Schmelzer, L. Asbrink, and M. Jonsson, Chem. Phys. **49**, 213 (1980).
[49] P. J. Mukherjee and D. P. Chong, Chem. Phys. Lett. **86**, 190 (1982).
[50] W. von Niessen, L. Asbrink, and G. Bieri, J. Electron Spectrosc. Relat. Phenom. **26**, 173 (1982).
[51] C. R. Brundle, M. B. Robin, N. A. Kuebler, and H. J. Basch, J. Am. Chem. Soc. **94**, 1451 (1972).
[52] C. Fridh and L. Asbrink, J. Electron Spectrosc. Relat. Phenom. **7**, 119 (1975).
[53] L. Asbrink, A. Svensson, W. von Niessen, and G. Bieri, J. Electron Spectrosc. Relat. Phenom. **24**, 293 (1981).